http://dx.doi.org/10.5012/bkcs.2013.34.9.2640

Comparison of Oct-2-enyl and Oct-4-enyl Staples for Their Formation and α-Helix Stabilizing Effects

Thanh K. Pham, Jiyeon Yoo, and Young-Woo Kim*

*College of Pharmacy, Dongguk University, Seoul 100-715, Korea. *E-mail: ywkim730@dongguk.edu*
Received April 24, 2013, Accepted June 10, 2013

The all-hydrocarbon *i*,*i*+4 stapling system using an oct-4-enyl crosslink is one of the most widely employed chemical tools to stabilize an α-helical conformation of a short peptide. This crosslinking system has greatly extended our ability to modulate intracellular protein-macromolecule interactions. The helix-inducing property of the *i*,*i*+4 staple has shown to be highly dependent on the length and the stereochemistry of the oct-4-enyl crosslink. Here we show that changing the double bond position within the *i*,*i*+4 staple has a considerable impact not only on the formation of the crosslink but also on α-helix induction. The data further increases the understanding of the structure-activity relationships of this valuable chemical tool.

Key Words : α-Helix, Stapled peptides, Ring-closing metathesis, Protease resistance, Peptide drugs

Introduction

The α-helix is the most common secondary structure found in proteins and often plays a critical role in protein-macromolecule interactions in cells.[1] Therefore, a short stretch of a peptide mimicking an α-helix structure has the potential to modulate biomolecular recognition events.[2] Based on this notion, a variety of strategies to enforce short peptides to adopt the α-helical conformation *via* chemical modifications have been actively investigated.[3]

Among these strategies, the "all-hydrocarbon stapling" system, developed by Verdine and his colleagues,[4] has generated considerable interest within the scientific community. Because it combines two powerful helix-stabilizing elements, α,α-dialkylamino acids and their cross-linkage over one (*i*,*i*+3 or *i*,*i*+4) or two turns (*i*,*i*+7) of a helix (Figure 1), this system is highly effective in promoting an α-helix formation and greater cell-permeability in short peptides.[5] For this reason, with the exception of the recently developed *i*,*i*+3 version,[6] this stapling system has been widely applied to modulate intracellular protein-protein interactions that have been difficult to target using conventional approaches.[7]

In Verdine's original study, when the *i*,*i*+7 stapling system was applied to a RNase A model peptide sequence, it showed promising results in stabilizing the α-helical conformation compared to its *i*,*i*+4 counterpart.[4] However, when applied to the BH3 domain of the apoptotic effector protein BID, the *i*,*i*+4 stapling system also exhibited significant helix induction, greater than that produced by an *i*,*i*+7 staple.[8] The resulting *i*,*i*+4 stapled peptide SAHBa (**s**tabilized **α**-**h**elix of the **B**H3 domain of BID) suppressed the growth of highly aggressive human leukemia cells xenotransplanted into mice. After this remarkable *in vivo* demonstration of the *i*,*i*+4 stapling system as a useful chemical tool for developing a novel class of peptide therapeutics, it has been widely applied to several other systems.[9]

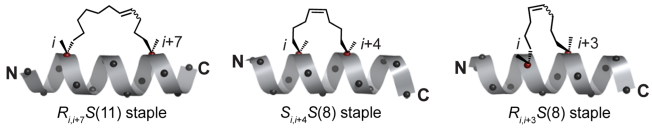


Figure 1. Three stapling systems in a schematic presentation. The nomenclature $R_{i,i+7}S(11)$ refers to an 11-carbon metathesized crosslink with the *R*-configuration at *i* and the *S*-configuration at *i*+7 position; $S_{i,i+4}S(8)$, 8-carbon tether with the *S*-configuration at both *i* and *i*+4 positions; $R_{i,i+3}S(8)$, 8-carbon tether with the *R*-configuration at *i* and the *S*-configuration at *i*+3.

Continuing reports of positive data regarding *i*,*i*+4 stapling have urged systematic studies focusing on elaborating the structure-activity relationships of the *i*,*i*+4 staple. In their original and follow-up studies, Verdine and colleagues systematically investigated the effects of the stereochemistry and the length of the *i*,*i*+4 staple, and demonstrated that an 8-atom hydrocarbon crosslink with the *S*-configuration at both the *i* and *i*+4 positions, termed $S_{i,i+4}S(8)$, is the most optimal in terms of both crosslinking efficiency and helix stabilizing effect.[4,10] In practice, $S_{i,i+4}S(8)$ can be formed through the incorporation of two units of (*S*)-α-methyl,α-petenylglycine (***S*****5**) (Figure 2(b)) into a peptide at the relative positions *i* and *i*+4, followed by ruthenium-mediated ring-closing metathesis (RCM). The resulting $S_{i,i+4}S(8)$ staple is an oct-4-ene hydrocarbon, which bears the *cis*-olefin moiety in the center.[9e] Identifying another structure-activity relationship of the *i*,*i*+4-staple, we became interested in the potential impact of the olefin position within the $S_{i,i+4}S(8)$ staple on helix stabilizing effects. A different location of the olefin moiety may cause a different torsional strain in the hydrocarbon staple that would consequently affect the helix stabilizing effects of a staple. As an ongoing effort to delve deeper into this issue, here we report our study on the comparison of an oct-2-enyl crosslink to the original oct-4-enyl staple for the efficiency of chemical formation and α-helix induction.

Table 1. Sequences and metathesis reactions of peptide substrates, percent helicity and protease resistance of stapled peptides

Entry	Substrates		% Conversion[a] after 2 h-RCM[b]		Products[c]	
	Code	Sequence	rt	60 °C	Code	% Helicity[d]
1	***S*$_3$-*S*$_7$**	EWA***S*$_3$**TAA***S*$_7$**KFLAAHA	No reaction[e]	> 95%	***S*$_{i,i+4}$*S*(8)-Δ2**	49%
2	***S*$_7$-*S*$_3$**	EWA***S*$_7$**TAA***S*$_3$**KFLAAHA	No reaction[e]	Decomposed[f]	***S*$_{i,i+4}$*S*(8)-Δ6**	N/A[g]
3	***S*$_5$-*S*$_5$**	EWA***S*$_5$**TAA***S*$_5$**KFLAAHA	90%	N/A[g]	***S*$_{i,i+4}$*S*(8)-Δ4**	77%
4	**WT**	EWAETAAAKFLAAHA	N/A[g]	N/A[g]	**WT**	30%

[a]RCM product/(RCM product + starting material) as determined by reverse-phase high-performance liquid chromatography following cleavage from resin. [b]Metathesis was conducted on resin with the fully protected substrates in the presence of Grubbs first generation catalyst (20 mol %). [c]All the products were *N*-terminally acetylated and *C*-terminally amidated. [d]% Helicities were calculated from mean-residue ellipticities at 222 nm ($[\theta]_{222}$) using $-31{,}500(1\text{-}2.5/n)$ and 0 deg cm^2 dmol^{-1} as the values for 100 and 0% helicity, respectively; n is the number of amino acid residues in the peptide. [e]RCM products were not detected. [f]Starting material was consumed without producing the corresponding RCM products. [g]Not applicable.

Experimental

General. Commercially available solvents and reagents were used as received. All Fmoc-protected α-amino acids (except the olefinic amino acids, Fmoc-*S*$_5$-OH, Fmoc-*S*$_3$-OH, and Fmoc-*S*$_7$-OH), 2-(6-chloro-1-*H*-benzotriazole-1-yl)-1,1,3,3-tetramethylaminium hexafluorophosphate (HCTU), 6-chloro-benzotriazole-1-yloxy-tris-pyrrolidinophosphonium hexafluorophosphate (PyClock), and Rink Amide MBHA resin were purchased from NovaBiochem. Piperidine, *N*-methyl-2-pyrrolidinone (NMP), dimethylformamide (DMF), *N,N*-diisopropylethylamine (DIEA), Grubbs 1st generation catalyst (bis(tricyclohexylphosphine)benzylidine ruthenium (IV) dichloride), 1,2-dichloroethane (DCE), triisopropylsilane (TIS), and trifluoroacetic acid (TFA) were purchased from Sigma-Aldrich. Olefinic amino acids were purchased from Okeanos Tech Co. Ltd.

Peptide Synthesis. The peptides shown in Table 1 were prepared using Fmoc chemistry on Rink Amide MBHA resin with a loading capacity of 0.6 mmol/g.[5a] The dry resin (50 mg, 30 μmol) was swelled in NMP for 10 min before using. The Fmoc protecting group was removed by treatment with 25% piperidine in NMP (2 × 10 min). Natural amino acids were coupled for 30 min using HCTU as an activating agent (4.75 equiv.), 5 equiv. of Fmoc-protected amino acid, and 10 equiv. of DIEA in NMP. The coupling of olefinic amino acids was conducted for 2 h with Fmoc-protected amino acid (3 equiv.), PyClock (3 equiv.), and DIEA (6 equiv.). After each coupling or deprotecting reaction, the resin was washed with dichloromethane (DCM) (1 × 2 min), NMP (1 × 2 min), DCM (1 × 2 min), and NMP (1 × 2 min).

Metathesis and Purification. Ring-closing metathesis of resin-bound *N*-Fmoc, side-chain protected peptides was performed using 20 mol % of Grubbs I catalyst in degassed DCE for 2 h at room temperature or 60 °C. The reactions were monitored by liquid chromatography-mass spectrometry (LC/MS) after cleavage of the peptides from a resin aliquot. After draining the reaction solution, the resin was washed with DCE (3 × 2 min) and then with DCM (3 × 2 min). After the final Fmoc-deprotection reaction, the *N*-terminal amino group was treated with 30 equiv. of acetic anhydride and 60 equiv. of DIEA in NMP for 45 min. Resin was washed with DCM (3 × 2 min) and DMF (3 × 2 min) and dried *in vacuo* overnight. The peptides were deprotected and cleaved from the resin by treating them with a mixture of TFA/TIS/water (95/2.5/2.5) for 2 h, and precipitated by adding a 1:1 mixture of *n*-pentane and diethyl ether. The precipitate was collected by centrifugation, dissolved in a 1:1 mixture of acetonitrile and water, and filtered to remove resin. The products were purified through reverse phase high-performance liquid chromatography using a Zorbax C18 column (Agilent, 5 μm, 9.4 × 250 mm), and then LC/MS (Agilent, API4000).

Peptide WT. ESIMS *m/z* for $C_{75}H_{110}N_{20}O_{21}$ $[M+2H]^{2+}/2$ calcd 814.4, found 814.7.

Peptide S*$_{i,i+4}$*S(8)-2. ESIMS *m/z* for $C_{81}H_{120}N_{20}O_{19}$ $[M+2H]^{2+}/2$ calcd 839.5, found 840.0.

Peptide S*$_{i,i+4}$*S(8)-4. ESIMS *m/z* for $C_{81}H_{120}N_{20}O_{19}$ $[M+2H]^{2+}/2$ calcd 839.5, found 839.5.

Circular Dichroism. The peptides were dissolved in a 25 mM potassium phosphate buffer solution (pH 6.5). The concentrations were determined by absorbance spectroscopy at 280 nm (extinction coefficient for tryptophan, $\lambda_{280} = 5690$ cm^{-1}). Circular dichroism spectra were collected on a Chirascan HP dual polarization circular dichroism spectrometer with a temperature controller using the following standard measurement parameters: 1 nm step resolution, 3 accumulations, 0.5 sec response, 1 nm bandwidth, and 0.1 cm path length. All spectra were converted to a uniform scale of molar ellipticity after background subtraction. The curves were smoothed using standard parameters.

Results and Discussion

To investigate the positional effects of the olefin moiety within the *S*$_{i,i+4}$*S*(8) staple on helix-inducing ability, we first prepared a panel of peptide substrates based on the RNase A-derived model sequence (EWAETAAAKFLAAHA) (Table 1). The substrate ***S*$_3$-*S*$_7$**, which possesses (*S*)-α-methyl,α-allylglycine (***S*$_3$**) and (*S*)-α-methyl,α-heptenylglycine (***S*$_7$**) at positions 4 and 8 respectively, was designed to introduce an oct-2-enyl staple ***S*$_{i,i+4}$*S*(8)-Δ2** (Figure 2(c)). Substrate ***S*$_7$-*S*$_3$**, which incorporates the same set of the amino acids, but with their positions switched, was designed to insert an oct-6-enyl staple ***S*$_{i,i+4}$*S*(8)-Δ6** (Figure 2(d)). For the purpose of comparison, we also prepared the corresponding unmodified

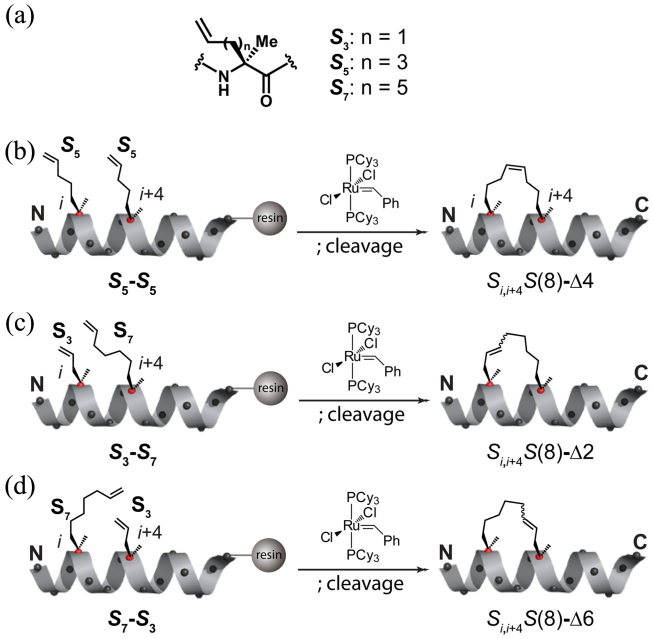


Figure 2. Structures of the three α-methyl, α-alkenylglycine units used in this study (A) and schematic representations of ring-closing metathesis reactions of peptide substrates incorporating a different set of α-methyl,α-alkenylglycine units leading to the formation of three isomeric octenyl crosslinks (B, C & D). The nomenclature $S_{i,i+4}S(8)$ refers to an 8-carbon metathesized cross-link with the *S*-configuration at *i* and *i*+4 positions. The number following Δ represents the position of the double bond within the octenyl crosslink; numbering starts from the *N*-terminal carbon.

peptide (**WT**) as well as substrate $\boldsymbol{S_5}$-$\boldsymbol{S_5}$, which contains $\boldsymbol{S_5}$ at both positions and would form the original *i*,*i*+4-staple, $\boldsymbol{S_{i,i+4}S(8)}$-**Δ4** (Figure 2(b)).

With all these peptide substrates prepared, we first examined the efficiency of the RCM reaction of each substrate. The fully-protected, resin-bound peptides were subjected to RCM under typical reaction conditions employed in previous studies, using 20 mol % of Grubbs first generation catalyst in 1,2-dichloroethane at room temperature for two h.[5a] To monitor the reaction progress temporally, an aliquot of resin was taken from each reaction at certain times during the 2 h RCM reaction, and the peptide material was released and analyzed using LC/MS. Intriguingly, under the given reaction conditions, neither substrate $\boldsymbol{S_3}$-$\boldsymbol{S_7}$ nor $\boldsymbol{S_7}$-$\boldsymbol{S_3}$ produced corresponding stapled products, whereas the conventional substrate $\boldsymbol{S_5}$-$\boldsymbol{S_5}$ underwent a smooth RCM to form its stapled product, showing a 90% conversion rate at the 2 h mark.

One of the important features of the all-hydrocarbon stapling strategy is that it exploits the templating effect induced by two helix-stabilizing elements: the Thorpe-Ingold effect induced by the incorporated α,α-dialkyl amino acids and the hydrophobic environment provided by the non-polar solvent promote α-helix formation of substrate peptides during the RCM reaction.[11,12] Since substrates are pre-organized into an α-helical conformation by this templating effect, it is not surprising that the stereochemistry and the length of olefin-

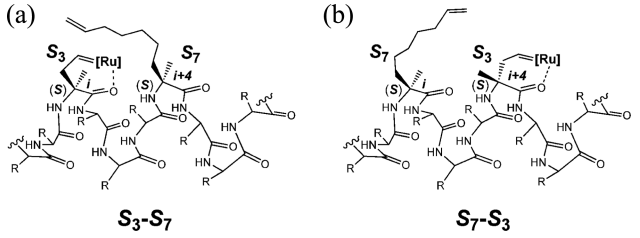


Figure 3. Chelate formation between the Ru-carbene of the allylic side-chain and the carbonyl oxygen of $\boldsymbol{S_3}$ unit as a plausible origin for the poor reactivity of the $\boldsymbol{S_3}$-containing peptides in an RCM reaction. The higher RCM efficiency of substrate $\boldsymbol{S_3}$-$\boldsymbol{S_7}$ at higher temperatures may be attributed to the favorable orientation of the Ru-carbene moiety during RCM with the olefin of the $\boldsymbol{S_7}$ side-chain.

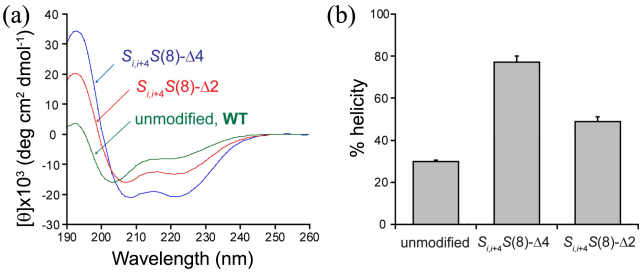


Figure 4. Circular dichroism spectra measured at 20 °C (a) and percent helicity (b) of the unmodified RNase A peptide (green) and its $\boldsymbol{S_{i,i+4}S(8)}$-**Δ2** (red) and $\boldsymbol{S_{i,i+4}S(8)}$-**Δ4** (blue) stapled analogs. Error bars represent the mean ± standard deviation of two independent experiments. % Helicities were calculated from mean-residue ellipticities at 222 nm ($[\theta]_{222}$) using −31,500(1-2.5/*n*) and 0 deg cm^2 dmol^{-1} as the values for 100 and 0% helicity, respectively; *n* is the number of amino acid residues in the peptide.

bearing side-chains play a critical role for favorable RCM reactions, since they are key elements for placing the two olefins in fairly close proximity. Considering that all three substrates would form *i*,*i*+4-staples of the same stereochemistry and length, the poor reactivity of substrates $\boldsymbol{S_3}$-$\boldsymbol{S_7}$ and $\boldsymbol{S_7}$-$\boldsymbol{S_3}$ in RCM may be attributed to the allyl group; the olefin group of the relatively small allyl group may be sterically too crowded for the Ru catalyst, or the Ru-carbene complex of $\boldsymbol{S_7}$ unit (if RCM is initiated with $\boldsymbol{S_7}$ unit) to access it.[13] Another plausible explanation is that even if the Ru catalyst can reach the allyl group, then the resulting Ru-carbene complex may form a stable chelate by coordinating to the carbonyl oxygen of $\boldsymbol{S_3}$ (Figure 3),[14] which would make it difficult to undergo a metathesis reaction with $\boldsymbol{S_7}$ under the given conditions. In addition, the stapled products formed from the three substrates would only differ in the position of the double bond within the 8-carbon tether. Therefore, we cannot completely ignore the possibility that the torsional strains caused by $\boldsymbol{S_{i,i+4}S(8)}$-**Δ2** and $\boldsymbol{S_{i,i+4}S(8)}$-**Δ6** staples may not be favorable for α-helix stabilization.

In an attempt to promote product formation of substrates $\boldsymbol{S_3}$-$\boldsymbol{S_7}$ and $\boldsymbol{S_7}$-$\boldsymbol{S_3}$ in RCM, we next explored new reaction conditions by manipulating temperature as many studies employed elevated temperatures for allyl-containing substrates in RCM reactions.[13b,15] When the RCM reactions were

performed at 60 °C, substrate S_3-S_7 underwent RCM yielding a single corresponding stapled product whose olefin geometry is yet to determined. Interestingly, substrate S_7-S_3 did not afford the stapled product but instead appeared to be degraded. Considering that substrate S_3-S_7 and S_7-S_3 only differ in the relative positions of the allyl and heptenyl groups, this result indicates that the relative positions of this specific set of olefinyl side-chains are another critical factor for effective RCM. For the two olefin groups to be placed in close proximity favorable for RCM, the side-chain at position *i* must bend toward the *C*-terminus while that of position *i*+4 must project toward the *N*-terminus on an α-helical peptide template. There are two plausible explanations. First, if the metathesis is initiated with the shorter S_3 side-chain, the Ru-carbene moiety of S_3 must be separated from the chelation with the carbonyl oxygen to participate in metathesis with S_7 olefin. In the case of substrate S_3-S_7, the Ru-carbene is already bent toward the *C*-terminus due to the chelation, which is favorable for the metathesis reaction with the S_7 (Figure 3(a)). However, for substrate S_7-S_3, the chelation places the Ru-carbene of S_3 at the *i*+4 position in the opposite direction, and therefore it would pose a much higher energy barrier to overcome for the metathesis reaction to occur (Figure 3(b)). In addition, it is also possible that the $S_{i,i+4}S$**(8)-Δ6** staple formed by S_7-S_3 simply causes less favorable torsional strains for helix stabilization compared to those induced by $S_{i,i+4}S$**(8)-Δ2**. Further studies are required to analyze these trends in detail.

To examine the conformational consequence of introducing $S_{i,i+4}S$**(8)-Δ2** in comparison to the original $S_{i,i+4}S$**(8)-Δ4** counterpart, we measured the far ultraviolet circular dichroism spectra under an aqueous environment. We avoided using trifluoroethanol, or other organic solvents, since they have helix-inducing properties. The stapled peptide constrained by $S_{i,i+4}S$**(8)-Δ2** clearly showed a notable increase in helical content (49% helicity) compared to the unmodified control **WT** (30% helicity) (Figure 4).[16] However, its helical content was much lower than that of a stapled peptide bearing the original $S_{i,i+4}S$**(8)-Δ4** staple (77% helicity). These results clearly showed that the RCM efficiency of olefin-bearing peptide substrates can reflect the extent of helix stabilization by the corresponding metathesized crosslink and, more importantly, that the position of double bond within the 8-carbon staple has a considerable effect on the helix inducing property of the crosslink. Further systematic studies are required to elucidate the detailed mechanism of this phenomenon.

Conclusion

In this study, we have demonstrated that the chemical formation and the helix inducing properties of an octenyl staple are greatly affected by the position of the double bond in the crosslink. The results obtained from this study confirm that Verdine's original (*S*,*S*)-configured oct-4-enyl staple, which has been the most widely employed in biological settings, is the most effective *i*,*i*+4 stapling system in enforcing a peptide into an α-helical conformation. We believe that the data provided from this study will serve as an important step forward in better understanding of the structure-activity relationships of this valuable all-hydrocarbon stapling system.

Acknowledgments. This research was supported by the Dongguk University Research Fund of 2011.

References

1. Creighton, T. E. *Proteins: Structures and Molecular Properties*; Freeman and Co.: New York, 1984.
2. Fairlie, D. P.; West, M. L.; Wong, A. K. *Curr. Med. Chem.* **1998**, *5*, 29-62.
3. (a) Marqusee, S.; Baldwin, R. L. *Proc. Natl. Acad. Sci. USA* **1987**, *84*, 8898-8902. (b) Ghadiri, M. R.; Choi, C. *J. Am. Chem. Soc.* **1990**, *112*, 1630-1632. (c) Kemp, D. S.; Allen, T. J.; Oslick, S. L. *J. Am. Chem. Soc.* **1995**, *117*, 6641-6657. (d) Osapay, G.; Taylor, J. W. *J. Am. Chem. Soc.* **1990**, *112*, 6046-6051. (e) Jackson, D. Y.; King, D. S.; Chmielewski, J.; Singh, S.; Schultz, P. G. *J. Am. Chem. Soc.* **1991**, *113*, 9391-9392. (f) Kumita, J. R.; Smart, O. S.; Woolley, G. A. *Proc. Natl. Acad. Sci.* **2000**, *97*, 3803-3808. (g) Cabezas, E.; Satterthwait, A. C. *J. Am. Chem. Soc.* **1999**, *121*, 3862-3875. (h) Cantel, S. *et al*. *J. Org. Chem.* **2008**, *73*, 5663-5674. (i) Blackwell, H. E.; Sadowsky, D. J.; Howard, R. J.; Sampson, J. N.; Chao, J. A.; Steinmetz, W. E.; O'Leary, D. J.; Grubbs, R. H. *J. Org. Chem.* **2001**, *66*, 5291-5302. (j) Chapman, R. N.; Dimartino, G.; Arora, P. S. *J. Am. Chem. Soc.* **2004**, *126*, 12252-12253. (k) Lim, Y.-B.; Moon, K. S.; Lee, M. *Angew. Chem. Int. Ed.* **2009**, *48*, 1601-1605.
4. Schafmeister, C. E.; Po, J.; Verdine, G. L. *J. Am. Chem. Soc.* **2000**, *122*, 5891-5892.
5. (a) Kim, Y.-W.; Grossmann, T. N.; Verdine, G. L. *Nat. Proc.* **2011**, *6*, 761-771. (b) Kutchukian, P. S.; Yang, J. S.; Verdine, G. L. Shakhnovich, E. I. *J. Am. Chem. Soc.* **2009**, *131*, 4622-4627.
6. Kim, Y.-W.; Kutchukian, P. S.; Verdine, G. L. *Org. Lett.* **2010**, *12*, 3046-3049.
7. For recent reviews, see: (a) Verdine, G. L.; Walenski, L. D. *Clin. Cancer Res.* **2007**, *13*, 7264-7270. (b) Verdine, G. L.; Hilinski, G. J. *Methods Enzymol.* **2012**, *503*, 3-33. (c) Verdine, G. L.; Hilinski, G. J. *Drug Discov. Today* **2012**, *9*, e41-e47.
8. Walensky, L. D.; Kung, A. L.; Escher, I.; Malia, T. J.; Barbuto, S.; Wright, R. D.; Wagner, G.; Verdine, G. L.; Korsmeyer, S. J. *Science* **2004**, *305*, 1466-1470.
9. (a) Danial, N. N; Walensky, L. D.; Zhang, C. Y.; Choi, C. S.; Fisher, J. K.; Molina, A. J. *et al*. *Nat. Med.* **2008**, *14*, 144-153. (b) Gavathiotis, E.; Suzuki, M.; Davis, M. L.; Pitter, K.; Bird G. H.; Katz, S. G.; Tu, H.-G.; Cheng, E. H.-Y.; Tjandra, N.; Walensky, L. D. *Nature* **2008**, *455*, 1076-1081. (c) Moellering, R. E.; Cornejo, M.; Davis, T. N.; Bianco, C. D.; Aster, J. C. *et al*. *Nature* **2009**, *462*, 182-188. (d) Zhang, H.; Zhao, Q.; Bhattacharya, S.; Waheed, A. A.; Tong, X.; Hong, A.; Heck, S.; Curreli, F.; Goger, M.; Cowburn, D.; Freed, E. O.; Debnath, A. K. *J. Mol. Biol.* **2008**, *278*, 565-580. (e) Phillips, C.; Roberts, L. R.; Schade, M.; Bazin, R.; Bent, A. *et al*. *J. Am. Chem. Soc.* **2011**, *113*, 9696-9699. (f) Chapuis, H.; Slaninová, J.; Bednárová, L.; Monincová, L.; Buděšínský, M.; Čeřovský, V. *Amino Acids* **2012**, *43*, 2047-2058.
10. Kim, Y.-W.; Verdine, G. L. *Bioorg. Med. Chem. Lett.* **2009**, *19*, 2533-2536.
11. Toniolo, C.; Crisma, M.; Formaggio, F.; Peggion, C. *Biopolymers* **2001**, *60*, 396-419.
12. Urnes, P.; Doty, P. *Adv. Protein Chem.* **1961**, *16*, 401-544.
13. (a) Biagini, S. C. G.; Gibson, S. E.; Keen, S. P. *J. Chem. Soc. Perkin Trans. 1* **1998**, 2485-2499. (b) Lin, Y. A.; Chalker, J. M.; Davis, B. G. *ChemBioChem*. **2009**, *10*, 959-969. (c) Reichwein, J. F.; Versluis, C.; Liskamp, R. M. J. *J. Org. Chem.* **2000**, *65*, 6187-

6195.
14. Furstner, A.; Langemann, K. *Synthesis* **1997**, 792-803.
15. (a) Creighton, C. J.; Reitz, A. B. *Org. Lett.* **2001**, *3*, 893-895. (b) Stymiest, J. L.; Mitchell, B. F.; Wong, S.; Vederas, J. C. *Org. Lett.* **2003**, *5*, 47-49.
16. Chen, Y.-H.; Yang, J. T.; Martinez, H. M. *Biochemistry* **1972**, *11*, 4120-4131.
17. Tyndall, J. D.; Nall, T.; Fairlie, D. P. *Chem. Rev.* **2005**, *105*, 973-999.